MATERIALES DE CONSTRUCCIÓN
Vol. 69, Issue 336, October–December 2019, e202
ISSN-L: 0465-2746
https://doi.org/10.3989/mc.2019.03619

Acoustic behavior of porous concrete. Characterization by experimental and inversion methods

M. Pereira[a], J. Carbajo[b], L. Godinho[a], P. Amado-Mendes[a], D. Mateus[a], J. Ramis[b]✉

[a]ISISE, Department of Civil Engineering, University of Coimbra (Portugal)
[b]Department of Physics, Systems Engineering and Signal Theory, University of Alicante, San Vicente del Raspeig (Spain)
✉jramis@ua.es

Received 20 March 2019
Accepted 19 June 2019
Available on line 7 October 2019

ABSTRACT: The use of porous concrete solutions with lightweight aggregates has become increasingly common in noise control due to their versatility in exterior and interior applications. In this work, samples of porous consolidated concrete with aggregates of expanded clay were produced, in order to study the influence of the grain size, thickness and water/aggregate/cement ratio on the sound absorption. Experimental techniques were used to obtain the surface impedance and sound absorption coefficient. In addition to experimental characterizations, an inverse method was used (based on a genetic algorithm) to obtain the macroscopic parameters capable of representing the materials studied through the theoretical model of Horoshenkov-Swift. Using the theoretical Horoshenkhov-Swift model it becomes possible to represent these materials in numerical models as equivalent fluids.

KEYWORDS: Concrete; Aggregate; Mixture proportion; Characterization; Modelization

Citation/Citar como: Pereira, M.; Carbajo, J.; Godinho, L.; Amado-Mendes, P.; Mateus, D.; Ramis, J. (2019) Acoustic behavior of porous concrete–characterization by experimental and inversion methods. Mater. Construcc. 69 [336], e202 https://doi.org/10.3989/mc.2019.03619

RESUMEN: *Comportamiento acústico del hormigón poroso. Caracterización mediante métodos experimentales e inversos.* El uso de soluciones basadas en hormigón poroso con agregados ligeros se ha vuelto cada vez más común en el ámbito del control de ruido debido a su versatilidad en aplicaciones exteriores e interiores. En este trabajo, se han preparado muestras de hormigón poroso con agregados de arcilla expandida, para estudiar la influencia del tamaño de grano, el espesor y la relación agua / agregado / cemento en la absorción de sonido. Se han utilizado técnicas experimentales para obtener la impedancia superficial y el coeficiente de absorción de sonido. Además de las caracterizaciones experimentales, se ha aplicado un método inverso (basado en un algoritmo genético) para obtener los parámetros macroscópicos capaces de representar los materiales estudiados a través del modelo teórico de Horoshenkov-Swift. Mediante el modelo teórico de Horoshenkhov-Swift, es posible representar estos materiales en modelos numéricos como fluidos equivalentes.

PALABRAS CLAVE: Hormigón; Agregado; Proporción de Mezcla; Caracterización Acústica; Modelización Acústica.

ORCID ID: M. Pereira (https://orcid.org/0000-0003-2229-1825); J. Carbajo (https://orcid.org/0000-0001-6377-5709); L. Godinho (https://orcid.org/0000-0002-2989-375X); P. Amado-Mendes (https://orcid.org/0000-0003-2233-2383); D. Mateus (https://orcid.org/0000-0002-4130-4786); J. Ramis (https://orcid.org/0000-0003-3105-2770)

1. INTRODUCTION

Porous absorbent materials have been widely used in passive noise control and indoor acoustic treatment. These materials are composed of two phases, one solid and the other fluid (interstitial to the pores), with the dissipation of the sound energy occurring due to the interaction between these two phases (1).

Currently, porous materials, such as fibers and foams, are commonly used in commercial solutions because of their excellent sound absorption at high frequencies. However, for exterior applications, these materials require protection against environmental agents, and structural reinforcement (2). Because of these requirements, the interest for materials with adequate constructive characteristics for direct external application (e. g. in acoustic barriers for traffic noise mitigation) has increased over the last decades. An example of a porous absorbent material with appropriate structural characteristics is the porous concrete. In 2000, Magrini and Ricciardi (3) proposed the use of expanded clay in the production of porous concrete, and since then several studies with different applications have been performed. Actually, several studies have been carried out on the application of granular materials for sound absorption purposes (not only concrete-based ones), whether these materials are consolidated or not (4–19). The works by Vašina et al. (2), Asdrubali and Horoshenkov (4) and Carbajo et al. (9) are of particular relevance, revealing some expected values of the macroscopic parameters for materials based in expanded clay. Nevertheless, significant discrepancies are seen between the results shown in those works, and it becomes clear that no single value can be defined for the common macroscopic parameters of such materials. They also indicate the need for further research in this important field.

The prediction of the acoustic behavior of granular materials is possible due to a number of works carried out for derivation and formulation of the acoustic impedance of porous materials (19–22). These models are particularly useful since they allow the representation of these materials as equivalent fluids in numerical models (23–30), which is very convenient and generic since it facilitates its use in practical application simulations.

This work aims to contribute to the knowledge of the acoustical parameters and study the sound absorption behavior of consolidated cementitious granular materials made of expanded clay. For this purpose, a total of 18 samples (with 2 specimens per sample) with different grain size, thickness, and water/cement ratio were prepared out from three different mixtures.

The sound absorption coefficient was measured for all the samples using a normalized impedance tube method with the objective of identifying the influence of the grain size, of thickness and the water/cement ratio on their absorption performance.

The theoretical model of Horoshenkov and Swift (31) has been used here to represent the behavior of the tested porous materials, based on four parameters: air-flow resistivity, open porosity, tortuosity and the standard deviation of the pore size. These parameters are determined through two techniques: the first one is experimental and it is used to determine the open porosity; the second is based on the use of an inverse method, which, using the experimental data of the impedance tube characterization (surface impedance and absorption coefficient), allows obtaining the other three macroscopic parameters required.

The structure of the paper is as follows: Section 2 introduces the sample preparation process and their physical characteristics (e. g. grain size, dry density…); in Section 3, the methodology is presented, and the experimental methods and the theoretical model of Horoshenkov and Swift are described, along with a brief explanation of the inversion algorithm used to estimate the macroscopic parameters of the materials; in Section 4, results concerning the sound absorption coefficient and the inversely determined acoustical parameters of the samples under study are presented; finally, Section 5 describes the main conclusion of this work.

2. MATERIAL

Three different grain sizes of expanded clay were first selected and analyzed using a sieving procedure, where the granular material passes through a series of sieves of progressively smaller mesh size and the amount of material stopped by each sieve as the fraction of the whole mass is registered; this experimental characterization procedure is described in the standard NP EN 993-1:2000 (32). The used expanded clay granulates are presented in Figure 1, classified through the commercial names: '0–2 mm' (a), '2–4 mm' (b), and '3–8 mm' (c).

Figure 2 shows the experimental curves of grain size distribution, where the aggregate denominated 3–8 mm has the largest grains and the one named 0–2 mm the smallest. As can be observed, the grain size distribution is relatively compact for the three cases; although there is no direct correspondence between the sieving analysis results and the commercial designation, the latter ('0–2 mm', '2–4 mm' and '3–8 mm') will be adopted for simplicity.

Two different mixtures were prepared using cement, water, and these aggregates following the proportions summarized in Table 1. The first mixture has the smallest cement content (34.32%); the second mixture was prepared with a larger cement content (37.36%). Initially, the mixtures were prepared for all aggregates, and samples were then produced.

FIGURE 1. Morphology of the three grain sizes of expanded clay studied: (a) 0–2 mm, (b) 2–4 mm and (c) 3–8 mm.

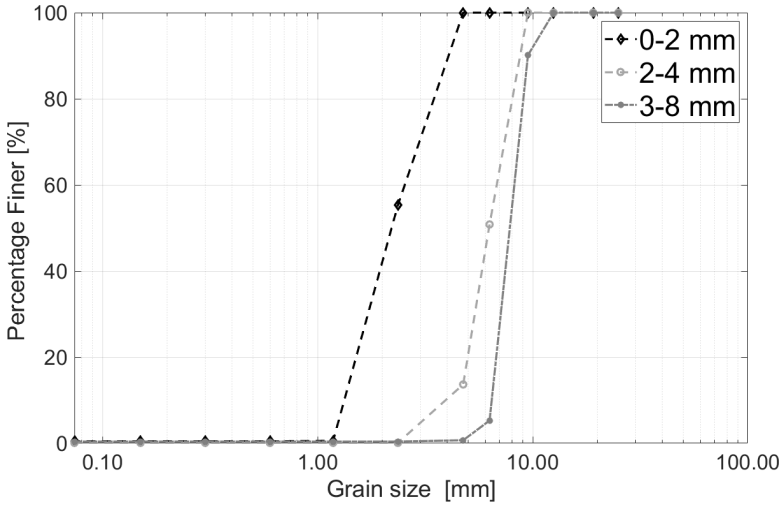

FIGURE 2. Grain size distribution obtained using the procedure described in NP EN 993-1:2000 (32).

However, for the smaller (0–2 mm) aggregate, the samples prepared with the first mixture were not sufficiently consolidated and desegregated easily. A third mixture was thus defined with 38.89% of cement, prepared only for the 0-2 mm aggregate.

Table 1 summarizes the mixtures preparation data and the thickness of the prepared samples. In this work, the samples were produced by mixing high strength Portland 42.5 cement, water and the necessary aggregates. The mixtures were poured into circular molds of different thickness (4, 6 and 8 cm) and with a cross section with diameter of 10.1 cm. Two specimens were produced for each thickness and for each tested combination of mixture and aggregate type, originating a total of 36 specimens (12 for Mixture 1, 18 for Mixture 2 and 6 for Mixture 3). After 48 h, the specimens are extracted from the molds to complete the cure over a period of 30 days. An image of some of the prepared specimens is depicted in Figure 3.

3. METHODS

3.1. Experimental methods

Three experimental methods were used to characterize the normal incidence acoustic properties of the prepared samples. The first method is described in ISO10534-2:2001(33), and allows the evaluation of the sound absorption using an impedance tube, based on the transfer function between two microphones, as indicated in the schematic representation of Figure 4. The impedance tube used in the present work has a circular cross-section with diameter of 10.1 cm, the cut-off frequency being approximately 1800 Hz. A random excitation is provided to the speaker from the analyzer OR34 Compact Analyzer, the sound pressure measured using two microphones B&K Type 4188 ½, and the pressure data post-processed in Matlab to obtain both the surface impedance and the sound absorption coefficient.

TABLE 1. Produced mixtures and samples (average of 2 specimens per sample)

Granular mixture	A/C/W*(%)	Commercial designation	Thickness (cm)	Average of volumetric mass density ρ (kg/m^3)
Mixture 1	48.48/34.32/	2–4	4	586.2
	17.20		6	618.1
			8	577.2
		3–8	4	587.8
			6	515.3
			8	496.0
Mixture 2	43.96/37.36/	0–2	4	656.0
	18.68		6	656.0
			8	670.6
		2–4	4	669.0
			6	711.2
			8	694.1
		3–8	4	643.0
			6	670.1
			8	604.0
Mixture 3	40.17/38.89/	0–2	4	816.8
	19.92		6	823.8
			8	697.4

*A/C/W indicates the Aggregate, Cement and Water proportions (in weight) of each mixture, respectively.

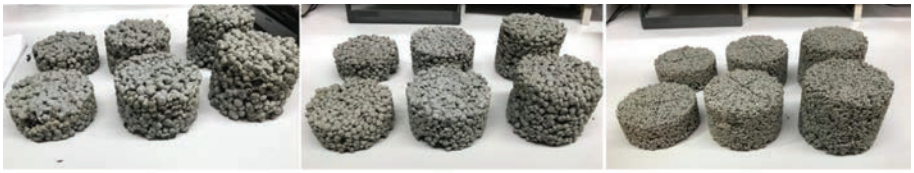

FIGURE 3. Images of some of the produced samples, with aggregates 3–8 mm (a), 2–4 mm (b) and 0–2 mm (c).

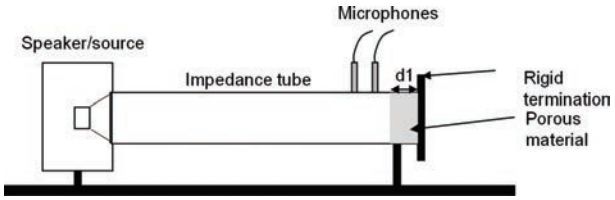

FIGURE 4. Experimental measurement apparatus used for the characterization of the prepared samples according to ISO 10534-2:2001 (33).

The surface impedance, Z_s , is calculated as [1]:

$$Z_s = \rho_0 c_0 \frac{(1+R)}{(1-R)}, \qquad [1]$$

where ρ_0 is the air density, c_0 is the sound propagation velocity in air, and R is the reflection coefficient, which is obtained from Equation [2], where s is the distance between the two microphones, x_1 is the distance between the sample and the microphone farther from the loudspeaker, $k_0=\omega/c_0$ is the wave number in air, being ω the angular frequency, and H^*_{12} is the transfer function between the two microphones incorporating the phase correction described in the standard,

$$R = \frac{H_{12}^* - e^{-jk_0 s}}{e^{jk_0 s} - H_{12}^*} e^{2jk_0 x_1} \qquad [2]$$

3.2. Theoretical Horoshenkov and Swift model

Several theoretical models can be used to predict the acoustic properties of porous materials. In this work, the model of Horoshenkov and Swift (31) for granular porous media was used, which is suitable for consolidated porous concrete samples, such

as the ones under study, and allows estimating the acoustic behavior from their macroscopic properties.

The present model considers four macroscopic parameters to determine the acoustic behavior, to list: air-flow resistivity, σ, open porosity, ϕ, tortuosity, α_∞ , and standard deviation of the pore size, σ_p. With these four macroscopic parameters, it is also possible to obtain the characteristic impedance and the wave number of the material for its representation in equivalent fluid models. This model was derived assuming rigid frame granular media with a log-normal pore size distribution. The intrinsic properties of the material can be represented by its complex density, ρ, and compressibility, C, calculated using the following equations [3] [4]

$$\rho = \frac{\alpha_\infty}{\phi}\left(\rho_0 - \frac{j\phi\sigma}{\omega\alpha_\infty}\tilde{\mathrm{F}}(\omega)\right), \qquad [3]$$

$$C = \frac{\phi}{\gamma \mathrm{P}_0}\left(\gamma - \frac{\rho_0(\gamma-1)}{\rho_0 - \mathrm{j}\dfrac{\sigma\phi}{\omega\alpha_\infty \mathrm{N}_{\mathrm{pr}}}\tilde{\mathrm{F}}\left(\mathrm{N}_{\mathrm{pr}}\omega\right)}\right), \qquad [4]$$

where γ is the ratio of specific heats, P_0 is the atmospheric pressure and N_{pr} is the Prandtl number, and $\tilde{F}$ is the viscosity correction function, which can be presented in the form of a Padé approximation as [5]:

$$\tilde{F}(\omega) = \frac{1 + a_1\epsilon + a_2\epsilon^2}{1 + b_1\epsilon}, \qquad [5]$$

where $a_1 = \theta_1/\theta_2$, $a_2 = \theta_1$ and $b_1 = a_1$. Considering a circular pore geometry assumption, $\theta_1 = \frac{4}{3}\mathrm{e}^{4\xi} - 1$ and $\theta_2 = \frac{\mathrm{e}^{3\xi/2}}{\sqrt{2}}$, where $\xi = \left(\sigma_p \ln(2)\right)^2$ and $\epsilon = \sqrt{\mathrm{j}\omega\rho_0\alpha_\infty / (\sigma\phi)}$ is a dimensionless parameter.

These parameters allow obtaining the characteristic impedance and complex wave number of the granular porous material by using the following expressions [6] [7]:

$$Z_{\mathrm{c}} = \sqrt{\rho / C} \qquad [6]$$

$$\mathrm{k} = \omega\sqrt{\rho C} \qquad [7]$$

3.3. Inverse characterization procedure

The macroscopic parameters required to represent the tested materials in the Horoshenkov and Swift model were obtained through an inversion method based on a genetic algorithm (34), where the objective function is obtained from the sum of quadratic error between the analytical and the experimental results, throughout the frequency domain. The only exception is the case of the open porosity, which was experimentally measured using the water saturation method. In this method, the open porosity is calculated from $\phi = V_f/V_t$, where V_f is the volume of fluid-space and V_t is the volume of the material sample. The volume of fluid-space is determined by $V_f = (M_{sat} - M_{dry})/\rho_{water}$, where M_{sat} is the mass of the sample saturated with water, M_{dry} is the mass of the dry sample, and ρ_{water} is the water density.

The air-flow resistivity, tortuosity and standard deviation of pore size were thus obtained using the referred inversion method. The inversion strategy used in this paper is based on the minimization of the difference between the experimental and the theoretical sound absorption coefficient, along a frequency range with *nf* discrete frequency values, and thus the objective function can be defined as [8]

$$OF(\omega) = \sum_{i=1}^{nf}\left|\alpha_{\mathrm{an}_i} - \alpha_{\mathrm{exp}_i}\right|^2 \qquad [8]$$

where α_{an_i} is the absorption coefficient obtained from the Horoshenkov and Swift model and α_{exp_i} is the experimental absorption coefficient.

Figure 5 presents a schematic representation of the procedure described. In the implementation of the inversion algorithm, it is important to define bounding limits for the calculation of the macroscopic parameters by the genetic algorithm. Indeed, these limits should be imposed in order to limit the search space of the algorithm and to ensure that the obtained parameters lie within the acceptable physical range for the type of material under study. The following limits are here considered:

- **Tortuosity**: The analytical expression proposed by Umnova et al. (35) which relates the open porosity and density to the tortuosity is used as a base for estimating the tortuosity. The acceptable variation range is assumed to be ±50% of the given value, which is defined as [9]

$$\alpha_\infty = 1 + \frac{1-\phi}{2\phi} \qquad [9]$$

It should be noted that values between 1.70 and 2.62 are observed in the works of Vašina et al. (2) or by Carbajo et al. (9).

- **Air-flow resistivity**: The variation of the amount of cement between mixtures is expected to greatly influence the air-flow resistivity of consolidated samples. Since most of the existing works (such as Umnova et al. (35)) present expressions for loose non-consolidated samples, these seem not to be adequate estimates in the context of the present paper. Based on the works

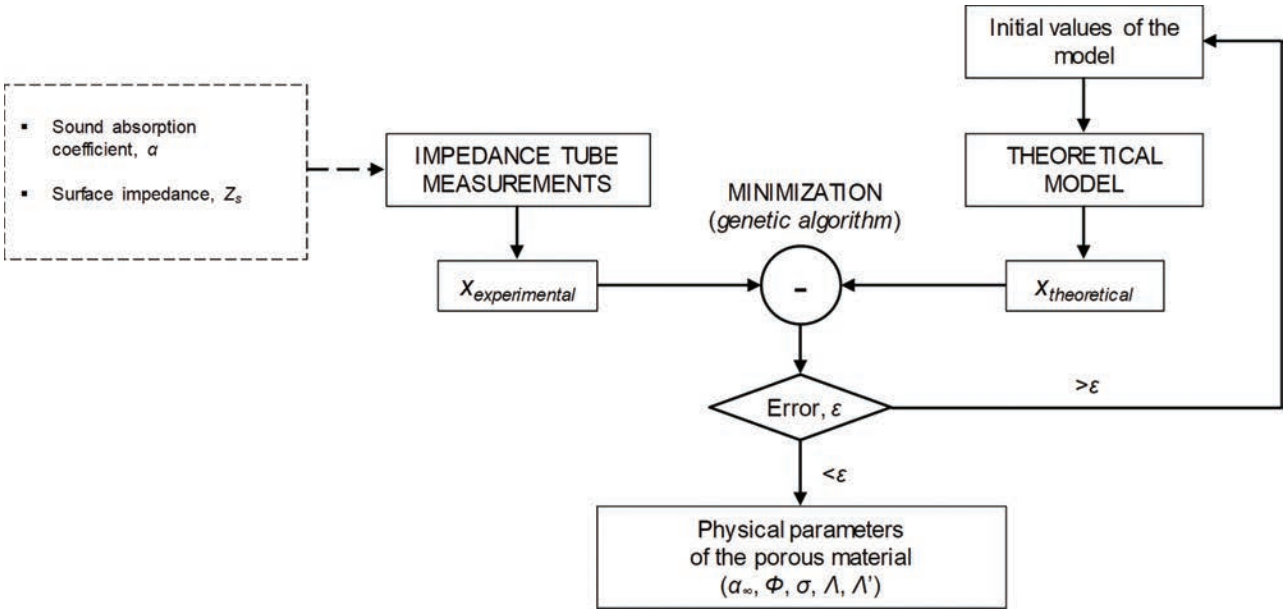

FIGURE 5. Schematic representation of the inversion procedure used for determining the macroscopic parameters.

of Vašina et al. (2) or by Carbajo et al. (9), it can also be seen that consolidated concrete samples can present a wide range of air-flow resistivity values, depending on the grain size and amount of cement, which greatly influence their acoustic behavior; Asdrubali and Horoshenkov (4) have even observed much larger values for this parameter (above 50000 $Pa.s/m^2$) in a specific case. Observing the values indicated in those works, a variation range from 1500 $Pa.s/m^2$ to 10000 $Pa.s/m^2$ was considered, to allow the algorithm to search in an extended space for optimal value.

- **Standard deviation of pore size**: For this parameter, the values indicated in Vašina et al. (2) and by Carbajo et al. (9) are quite different, and can range between 0.72 and 0.83 for the former, and between 0.16 and 0.24 for the latter. Given this large variation, the authors considered the extreme values of 0.16 and 0.83 as the interval limits for the standard deviation of pore size.

4. RESULTS AND DISCUSSION

In what follows, the results of the developed work are presented and analyzed. First, the results obtained by directly measuring the sound absorption coefficient in the impedance tube will be presented and discussed in order to understand the effect of the variation of a number of parameters, such as: grain size of the expanded clay aggregate, thickness of the sample and A/C/W relation of the mixture.

After that first analysis, results from the inversion process described in Section 3.3 are presented and discussed, assuming the material behavior to be described by the Horoshenkov and Swift model. The main objective is here to infer, using results from acoustic measurements, the macroscopic parameters of the different mixtures, so that simple equivalent fluid models can be used for their representation in numerical models.

4.1. Measured sound absorption coefficient

The experimental results concerning the impedance tube procedure described in the ISO 10534:2(33) for the prepared samples are here first presented, in order to allow analyzing the influence of grain size, thickness and amount of cement on the sound absorption of the specimens. Figures 6 to 8 illustrate the full set of sound absorption results measured for all produced samples. Each figure presents results obtained for the same aggregate, incorporating all measured sample thicknesses. Within each plot, results for the two mixtures used for the corresponding grain size are illustrated. Each curve corresponds to the result measured for a single sample type (averaged between the two specimens per sample).

Comparing samples made from the same aggregate and mixture, some common trends in the variation of the sound absorption coefficient can be observed as different thicknesses are considered. Indeed, for all mixtures, the increase of the thickness produces a shift in the absorption curve towards lower frequencies. This effect occurs for all

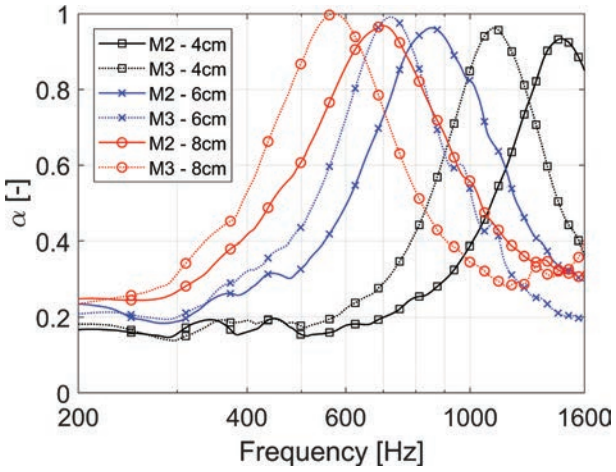

FIGURE 6. Sound absorption results measured in the impedance tube for samples with aggregate 0–2 mm, considering mixtures 2 and 3.

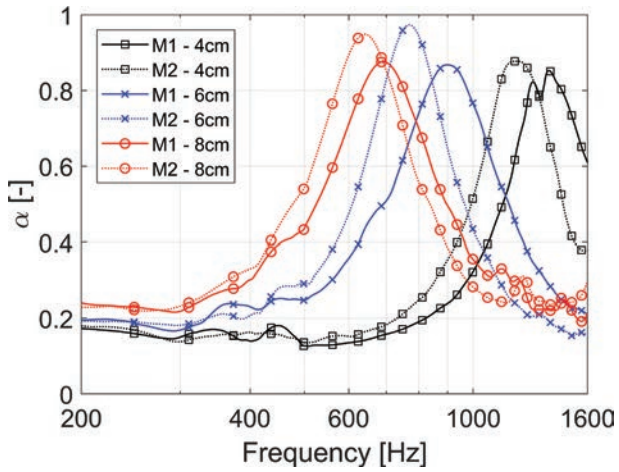

FIGURE 7. Sound absorption results measured in the impedance tube for samples with aggregate 2–4 mm, considering mixtures 1 and 2.

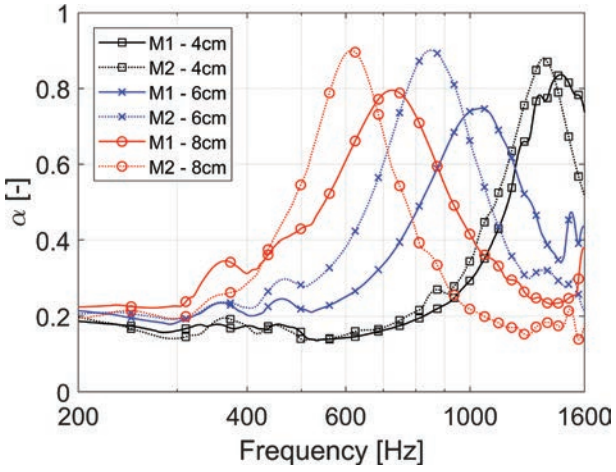

FIGURE 8. Sound absorption results measured in the impedance tube for samples with aggregate 3–8 mm, considering mixtures 1 and 2.

tested samples, regardless of the amount of cement or the grain size, and is a well-known and expected behavior.

If samples from mixture 2 and with the same thickness (either 4, 6 or 8 cm), but with varying grain size, are now compared, some interesting changes can be observed. It can be noted that a trend exists for the samples with smaller grain size to provide a somewhat broader sound absorption curve when compared with those made with aggregates of larger grain sizes. This can be seen quite clearly when comparing the 0–2 mm to both the 2–4 mm and 3–8 mm aggregates. When the 2–4 mm and 3–8 mm aggregates are compared, this relation is less evident.

It is also interesting to observe the results in terms of the influence of A/C/W proportions in the sound absorption, considering samples of different mixtures with the same thickness (4, 6 and 8 cm), and for each of the used grain size. Indeed, it can be noted that increasing the amount of cement provides a shift of the absorption peak to lower frequencies in all tested samples, as similarly observed when analyzing the influence of increasing the thickness of the samples. Samples with grain size 0–2 mm show the greatest variation, particularly when the 4 cm thick samples are analyzed. It is important to note that increasing the ratio of cement leads, in practice, to a denser sample, with more closed pores and internal channels, and thus to a change in some of its macroscopic parameters that influence the acoustic behavior.

Another interesting feature that can be observed is that as larger sized aggregates are considered (mostly for the 3–8 mm aggregate) there seems to be a sensible decrease of sound absorption peaks, which for the largest aggregate are always below 0.9 for mixture 2, and can be as low as 0.8 for mixture 1. A possible explanation for this behavior may be related to the larger dimension of the air-filled pores inside the sample, which may form paths with larger channels, and thus where lower viscous-thermal losses occur during the sound propagation process.

4.2. Macroscopic parameters

As stated at the beginning of this work, besides the characterization of the acoustic behavior of the different porous concrete mixtures, the main goal is to provide a better insight regarding the macroscopic parameters of this type of material. This is an important aspect that needs specific attention, since the knowledge of these parameters allows their simulation in theoretical models, such as those based on the concept of equivalent fluids. This section presents the results of the macroscopic parameters determined using the inverse procedure described in Section 3.3 for all the prepared specimens. As mentioned above, while the open porosity was determined experimentally, the other three parameters

(i.e. air-flow resistivity, tortuosity and the standard deviation of pore size) were determined through an inversion strategy.

The measured open porosity of the produced samples is presented in Table 2, where each value is the average of two samples with the same aggregate and mixture type. In all cases, values of the open porosity above 0.30 are registered, which are in line with the observations from other authors (see, for example, (2,9)). Within each type of material (i.e., samples with the same mixture and aggregate grain size), the observed values seem to be quite similar, with a variation of no more than 0.05 between samples of different thickness. As expected, the average value of the porosity tends to decrease as larger quantities of cement are considered; indeed, adding more cement allows to establish more internal connections between aggregate particles, reducing the open space between them. This can be seen clearly observing the corresponding values between mixtures 1 and 2 (the latter produced using more cement), and between mixtures 2 and 3 (again, the latter produced using more cement), for all aggregate types.

The inversion strategy defined before was applied independently to each produced sample, and the average values of the macroscopic parameters obtained for each of the mixtures and grain sizes are shown in Figures 9, 10 and 11, considering the average of all sample thicknesses, and two specimens of each type, for each case; thus, each value is an average of 6 samples. It should be noted that the inversion procedure was performed in the frequency range from 400 to 1600 Hz, in the attempt not to have the process affected by uncertainties of the experimental characterization which are mostly observed at lower frequencies.

Observing the estimated average values for the macroscopic parameters, some points should be mentioned. First, the values obtained for the air-flow resistivity (Figure 9) indicate that significant differences occur depending on the aggregate type considered. An important conclusion that can be inferred from the presented plot is that increasing the amount of cement leads to higher values of the air-flow resistivity; physically, this was an expected behavior, as the samples tend to have a more closed

TABLE 2. Measured open porosity (ϕ(-)) of the samples (average of the 2 specimens of each type)

Grain size		**3–8 mm**		**2–4 mm**		**0–2 mm**	
Mixture		**Mix. 1**	**Mix. 2**	**Mix. 1**	**Mix. 2**	**Mix. 2**	**Mix. 3**
	4 cm	0.37	0.33	0.39	0.36	0.48	0.38
Thickness	6 cm	0.39	0.33	0.36	0.31	0.46	0.33
	8 cm	0.38	0.34	0.38	0.35	0.45	0.37
Average ϕ		0.38	0.33	0.37	0.34	0.46	0.36

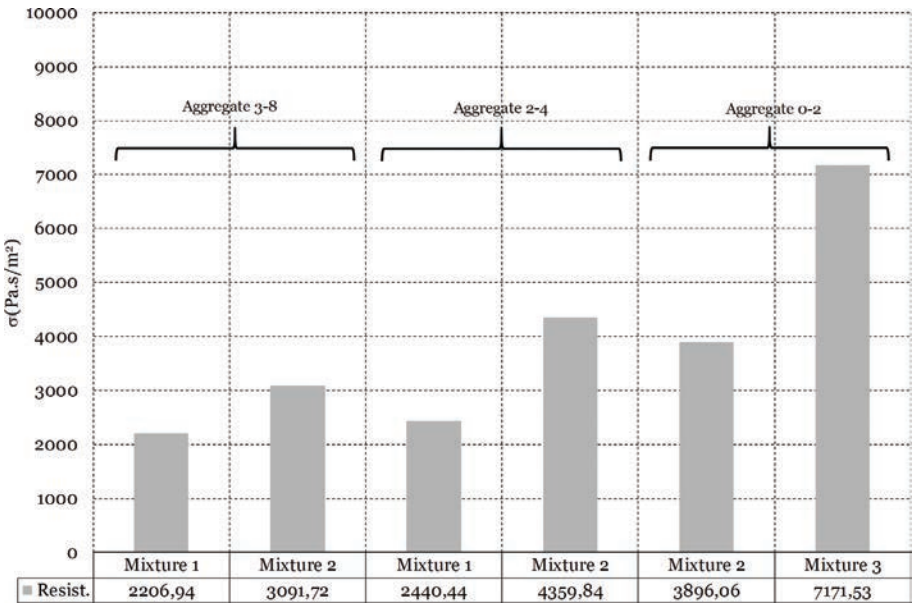

FIGURE 9. Average air-flow resistivity of the different mixtures and grain sizes obtained by inversion, considering the 6 sample types (12 specimens) produced for each case.

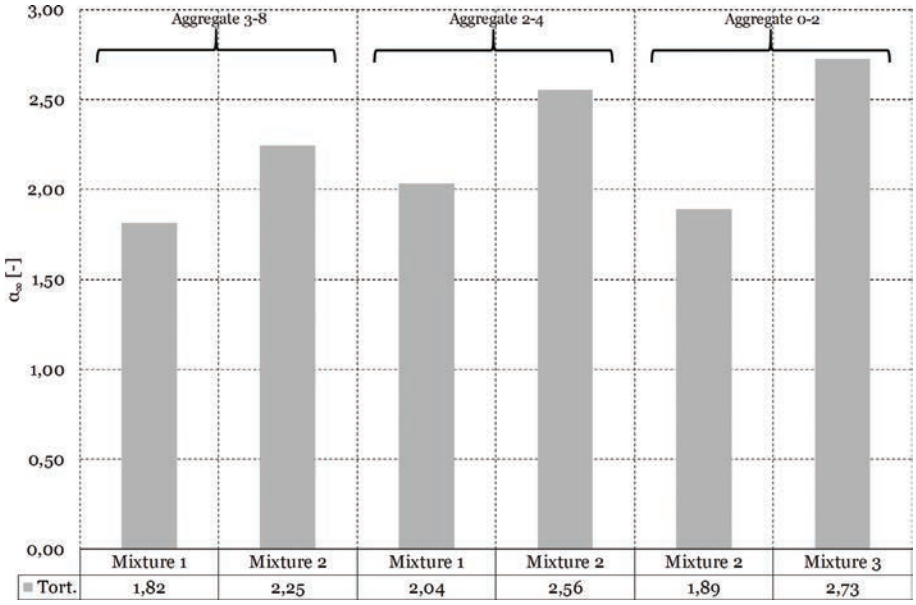

FIGURE 10. Average tortuosity of the different mixtures and grain sizes obtained by inversion, considering the 6 sample types (12 specimens) produced for each case.

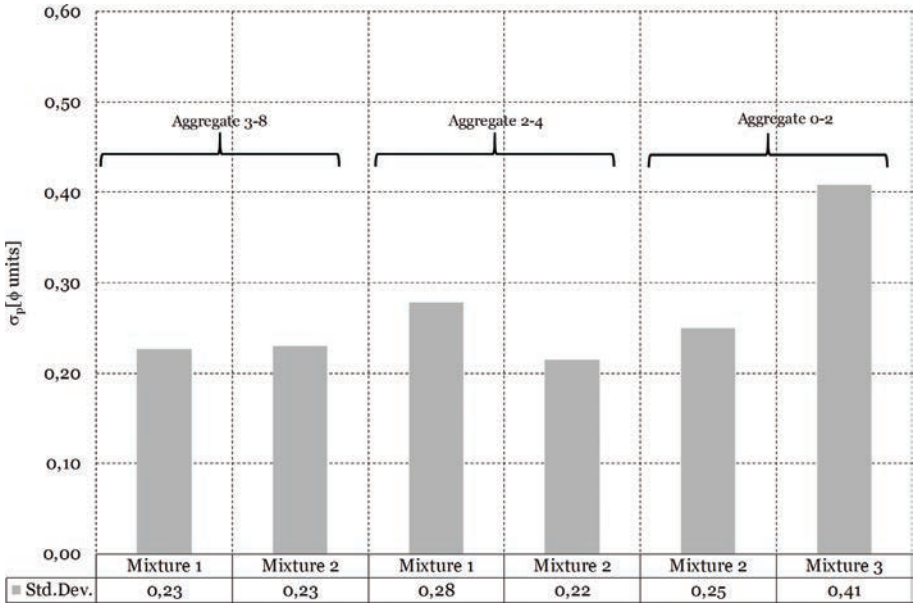

FIGURE 11. Average standard deviation of the pore size of the different mixtures and grain sizes obtained by inversion, considering the 6 sample types (12 specimens) produced for each case.

internal structure, with fewer voids and less open interstitial channels, making the air more difficult to flow. For the case of the tortuosity, the obtained values (Figure 10) are always above 1.80, which was an expected value for this type of material, while the standard deviation of pore size (Figure 11) ranged from 0.22 to 0.41, which are intermediate values between those given by Vašinaet al. (2) and Carbajo et al. (9). The presented estimations thus seem to be within the limits found in the literature for the tested materials.

In Figure 12 the full set of values for air-flow resistivity and tortuosity obtained by application of the inversion algorithm are displayed, as a function of density and of the ratio of the density to porosity, respectively; in the same plot, average values

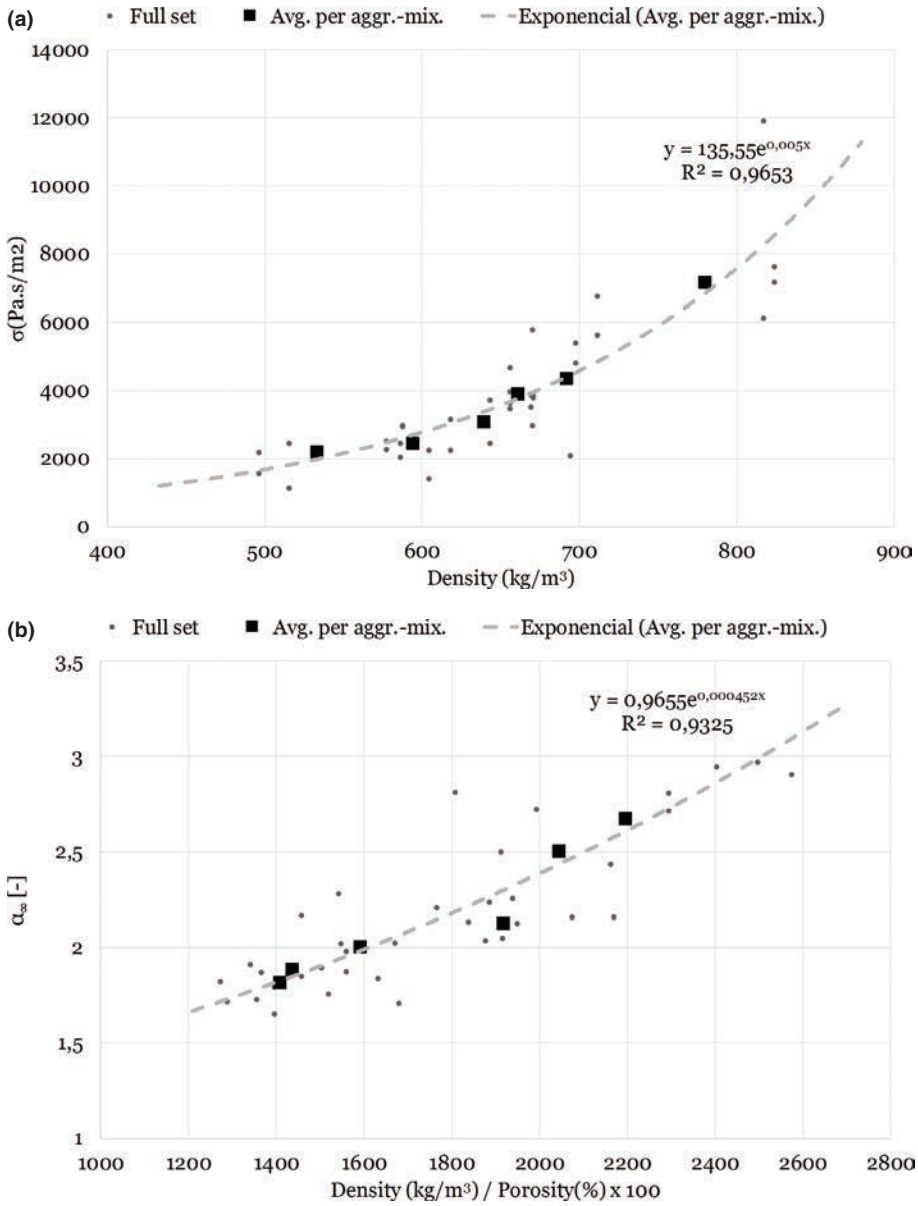

FIGURE 12. Estimated air-flow resistivity (a) and tortuosity (b) for all samples, and average values for each combination aggregate-mixture. Tendency lines are also displayed for each parameter.

calculated for each aggregate and mixture type are also displayed. The presented plots show significant dispersion when individual samples are analyzed, although a clear trend for the air-flow resistivity values to increase for higher sample densities can be seen in Figure 12a; similarly, the tortuosity seems to exhibit a similar trend as higher ratios density/porosity are considered. However, when average values per aggregate and mixture are analyzed these relations seem to become much more clear, and indeed a simple regression analysis considering an exponential curve exhibits a quite high correlation coefficient (R^2>0.93 for both cases), indicating that there is a strong relation between the correlated variables. Although a much larger number of samples would be needed for a statistically representative analysis, this initial study indicates that it may be possible to find a relation between the air-flow resistivity and density and between tortuosity and density to porosity ratio, that may allow to estimate air-flow resistivity and tortuosity from the density and porosity of the samples, which are quite simpler to evaluate experimentally.

Finally, to verify the application of the obtained parameters in reproducing the acoustic behavior of the tested samples, the plots in Figure 13 show

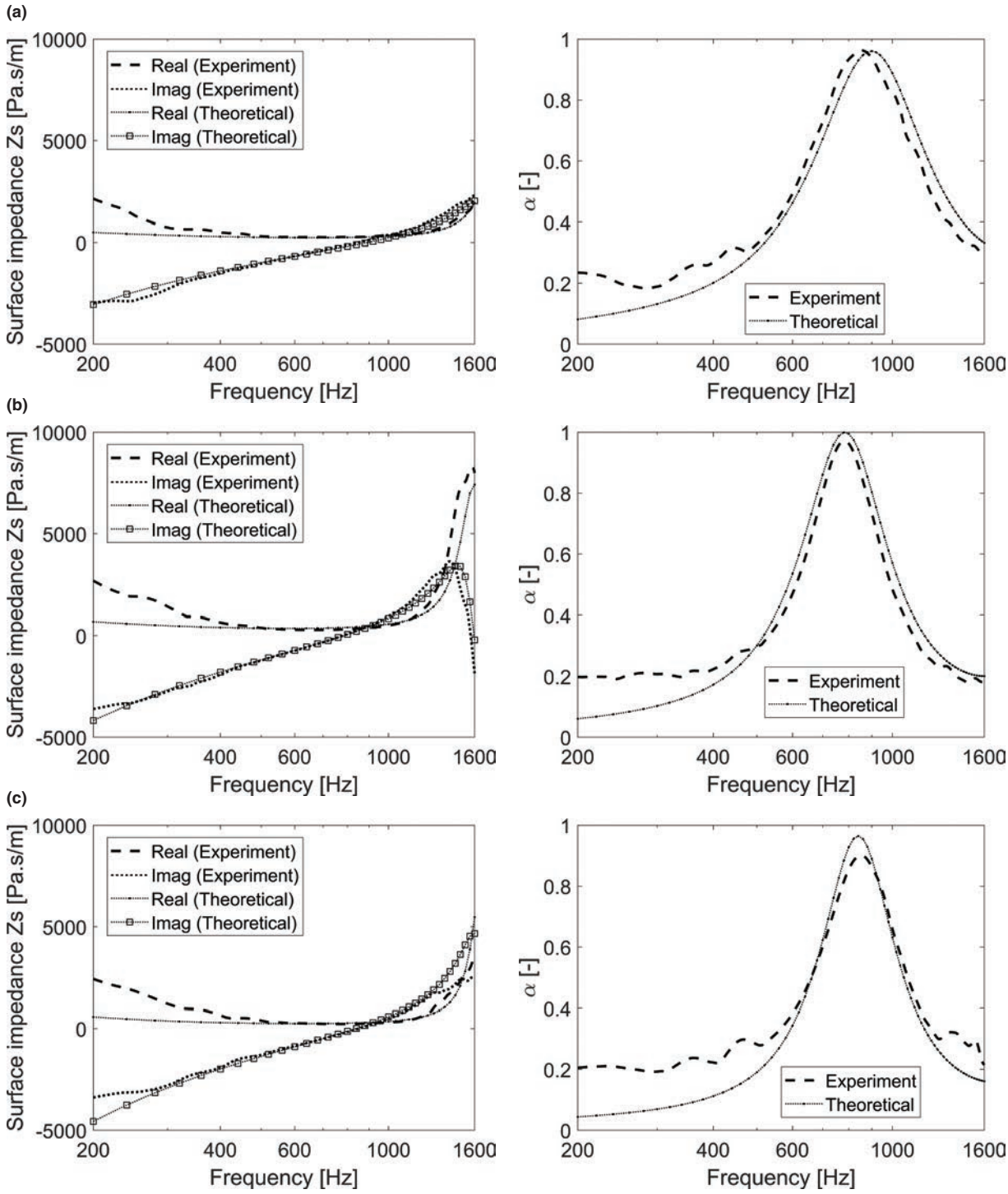

FIGURE 13. Comparison of the inversely determined and measured surface acoustic impedance (left) and sound absorption coefficient (right) for samples 6 cm thick and produced with Mixture 2: (a) 0–2 mm aggregate; (b) 2–4 mm aggregate; (c) 3–8 mm aggregate (Experimental values are average values of two specimens).

a comparison of the measured and calculated surface impedance and sound absorption coefficient for an illustrative case. For that purpose, the case of samples produced with Mixture 2 (which was used for all types of aggregates), and with a thickness of 6 cm is considered, for the three types of aggregates.

Observing the presented plots, it can be seen that a good approximation is provided by the theoretical

model, both in terms of surface impedance and of the sound absorption coefficient, although slightly overestimating the peak sound absorption for the larger-sizes aggregates. Indeed, for all plots the trend of the experimental measurements and the theoretical model is quite similar, although some differences are registered, mainly in the low frequency range and for the samples with the larger sized aggregates (2–4 mm and 3–8 mm). Observing the values of the sound absorption at the lowest frequencies, it becomes clear that quite high values are registered, with coefficients of 0.2 being registered at the lower frequency of 200 Hz. This value seems to be somewhat exaggerated comparing, for example, with the ones documented by Carbajo et al. (9) for similar materials, and may be related with the experimental conditions of this work. This low frequency behavior is not reproduced by the theoretical model, which estimated lower values of the sound absorption coefficient (and of the real part of the surface impedance).

5. CONCLUSIONS

The present paper gives a contribution to the study of the sound absorption properties of lightweight porous concrete, using expanded clay aggregates. Different aggregate sizes and proportions of water/cement/aggregate were used to produce test samples, and to allow studying the influence of different parameters in the acoustic behavior of the material. It was possible to identify a clear influence of the grain size and of the cement quantity in the acoustic absorption provided by the material, with the cement quantity playing a quite important role.

An inverse model was used, based on the theoretical equivalent-fluid representation proposed by Horoshenkov and Swift, based on the measured sound absorption coefficient. The obtained results seem to indicate that the approach leads to values of the macroscopic parameters of the material within the expected range (based on the literature). The presented results also show that there is a strong relationship between physical/macroscopic parameter (density, porosity, air-flow resistivity, tortuosity) and the amount of cement used in the preparation of the mixtures, for all sizes of aggregate grain. Finally, a simple regression analysis was proposed to correlate some of the macroscopic parameters (namely air-flow resistivity and tortuosity) with simpler physical properties (density and porosity), with good correlation being found between the tested variables. Establishing such correlations may be important for practical purposes, since porosity and density can be determined using simpler laboratorial procedures.

The results obtained in this work can facilitate the proposal and application of constructive solutions based in porous lightweight concrete to solve external acoustic problems.

ACKNOWLEDGMENTS

This work was developed within the scope of the POCI-01-0247-FEDER-033990 (iNBRail) Project, funded by FEDER funds through COMPETE 2020, Portugal 2020. This work was also supported by FEDER funds through the Competitivity Factors Operational Programme - COMPETE and by national funds through FCT – Foundation for Science and Technology within the scope of the project POCI-01-0145-FEDER-007633 and through the Regional Operational Programme CENTRO2020 within the scope of the project CENTRO-01-0145-FEDER-000006. The support of COST (European Cooperation in Science and Technology) through the COST Action CA15125 – DENORMS: "Designs for Noise Reducing Materials and Structures" is here also acknowledged.

REFERENCES

1. Fahy, F. J. (2000). *Foundations of engineering acoustics*. Elsevier.
2. Vašina, M.; Hughes, D. C.; Horoshenkov, K. V.; Lapčík Jr, L. (2006) The acoustical properties of consolidated expanded clay granulates. *Appl. Acoust.*, *67*[8], 787–796. https://doi.org/10.1016/j.apacoust.2005.08.003
3. Magrini, U.; Ricciardi, P. (2000) Surface sound acoustical absorption and application of panels composed of granular porous materials. *Proceedings of Inter-Noise 2000*, 27–30.
4. Asdrubali, F.; Horoshenkov, K. V. (2002) The acoustic properties of expanded clay granulates. *Build. Acoust.*, *9*[2], 85–98. https://doi.org/10.1260/135101002760164553
5. Krezel, Z. A.; McManus, K. (2000) Recycled aggregate concrete sound barriers for urban freeways. In *Waste Management Series, 1*, 884–892. https://doi.org/10.1016/S0713-2743(00)80097-5
6. Kim, H. K.; Lee, H. K. (2010) Influence of cement flow and aggregate type on the mechanical and acoustic characteristics of porous concrete. *Appl. Acoust.*, *71*[7], 607–615. https://doi.org/10.1016/j.apacoust.2010.02.001
7. Olek, J.; Weiss, W. J.; Neithalath, N. (2004) Concrete mixtures that incorporate inclusions to reduce the sound generated in portland cement concrete pavements, Report no. SQDH 2004-2, School of Civil Engineering, Purdue University.
8. Neithalath, N. (2004) Development and characterization of acoustically efficient cementitious materials, PhD Thesis, Purdue University.
9. Carbajo San Martín, J.; Esquerdo-Lloret, T. V.; Ramis-Soriano, J.; Nadal-Gisbert, A. V.; Denia, F. D. (2015) Acoustic properties of porous concrete made from arlite and vermiculite lightweight aggregates. *Mater. Construcc.* 65 [320], e072. http://dx.doi.org/10.3989/mc.2015.01115
10. Bartolini, R.; Filippozzi, S.; Princi, E.; Schenone, C.; Vicini, S. (2010) Acoustic and mechanical properties of expanded clay granulates consolidated by epoxy resin. *Appl. Clay. Sci.*, *48*[3], 460–465. https://doi.org/10.1016/j.clay.2010.02.007
11. Pereira, A.; Godinho, L.; Morais, L. (2010) The acoustic behavior of concrete resonators incorporating absorbing materials. *Noise Control Eng. J.*, *58*[1], 27–34. https://doi.org/10.3397/1.3264649
12. Kim, H. K.; Jeon, J. H.; Lee, H. K. (2012) Workability, and mechanical, acoustic and thermal properties of lightweight aggregate concrete with a high volume of entrained air. *Construc. Build. Mat.*, *29*, 193–200. https://doi.org/10.1016/j.conbuildmat.2011.08.067

13. Umnova, O.; Attenborough, K.; Shin, H. C.; Cummings, A. (2005) Deduction of tortuosity and porosity from acoustic reflection and transmission measurements on thick samples of rigid-porous materials. *Appl. Acoust.*, *66*[6], 607–624. https://doi.org/10.1016/j.apacoust.2004.02.005
14. Kim, H. K.; Lee, H. K. (2010) Acoustic absorption modeling of porous concrete considering the gradation and shape of aggregates and void ratio. *J. Sound Vib.*, *329*[7], 866–879. https://doi.org/10.1016/j.jsv.2009.10.013
15. Maderuelo-Sanz, R.; Nadal-Gisbert, A. V.; Crespo-Amorós, J. E.; Morillas, J. M. B.; Parres-García, F.; Sanchis, E. J. (2016) Influence of the microstructure in the acoustical performance of consolidated lightweight granular materials. *Acoust Aust*, *44*[1], 149–157. https://doi.org/10.1007/s40857-016-0048-5
16. Buratti, C.; Merli, F.; Moretti, E. (2017) Aerogel-based materials for building applications: Influence of granule size on thermal and acoustic performance. *Energ. Build.*, *152*, 472–482. https://doi.org/10.1016/j.enbuild.2017.07.071
17. Wang, H.; Ding, Y.; Liao, G.; Ai, C. (2016) Modeling and optimization of acoustic absorption for porous asphalt concrete. *J. Eng. Mech.*, *142*[4], 04016002. https://doi.org/10.1061/(ASCE)EM.1943-7889.0001037
18. Cobo, P.; Simón, F. (2016). A comparison of impedance models for the inverse estimation of the non-acoustical parameters of granular absorbers. *Appl. Acoust.*, *104*, 119–126. https://doi.org/10.1016/j.apacoust.2015.11.006
19. Attenborough, K. (1983) Acoustical characteristics of rigid fibrous absorbents and granular materials. *J. Acoust. Soc. Am.*, *73*[3], 785–799. https://doi.org/10.1121/1.389045
20. Miki, Y. (1990) Acoustical properties of porous materials-generalizations of empirical models. *J. Acoust. Soc. Jpn. (E)*, *11*[1], 25–28. https://doi.org/10.1250/ast.11.25
21. Stinson, M. R.; Champoux, Y. (1992) Propagation of sound and the assignment of shape factors in model porous materials having simple pore geometries. *J. Acoust. Soc. Am.*, *91*[2], 685–695. https://doi.org/10.1121/1.402530
22. Allard, J. F.; Champoux, Y. (1992) New empirical equations for sound propagation in rigid frame fibrous materials. *J. Acoust. Soc. Am.*, *91*[6], 3346–3353. https://doi.org/10.1121/1.402824
23. Panneton, R.; Atalla, N. (1996) Numerical prediction of sound transmission through finite multilayer systems with poroelastic materials. *J. Acoust. Soc. Am.*, *100*[1], 346–354. https://doi.org/10.1121/1.415956
24. Fouladi, M. H.; Nor, M. J. M.; Ayub, M.; Leman, Z. A. (2010) Utilization of coir fiber in multilayer acoustic absorption panel. *Appl. Acoust.*, *71*[3], 241–249. https://doi.org/10.1016/j.apacoust.2009.09.003
25. Tournat, V.; Pagneux, V.; Lafarge, D.; Jaouen, L. (2004) Multiple scattering of acoustic waves and porous absorbing media. *Phys. Rev. E*, *70*[2], 026609. https://doi.org/10.1103/PhysRevE.70.026609
26. Castagnede, B.; Aknine, A.; Brouard, B.; Tarnow, V. (2000) Effects of compression on the sound absorption of fibrous materials. *Appl. Acoust.*, *61*[2], 173–182. https://doi.org/10.1016/S0003-682X(00)00003-7
27. Glé, P.; Gourdon, E.; Arnaud, L. (2011) Acoustical properties of materials made of vegetable particles with several scales of porosity. *Appl. Acoust.*, *72*[5], 249–259. https://doi.org/10.1016/j.apacoust.2010.11.003
28. Bo, Z.; Tianning, C. (2009) Calculation of sound absorption characteristics of porous sintered fiber metal. *Appl. Acoust.*, *70*[2], 337–346. https://doi.org/10.1016/j.apacoust.2008.03.004
29. Sgard, F. C.; Atalla, N.; Nicolas, J. (2000) A numerical model for the low frequency diffuse field sound transmission loss of double-wall sound barriers with elastic porous linings. *J. Acoust. Soc. Am.*, *108*[6], 2865–2872. https://doi.org/10.1121/1.1322022
30. Xin, F. X.; Lu, T. J. (2010) Sound radiation of orthogonally rib-stiffened sandwich structures with cavity absorption. *Compos. Sci. Technol.*, *70*[15], 2198–2206. https://doi.org/10.1016/j.compscitech.2010.09.001
31. Horoshenkov, K. V.; Swift, M. J. (2001) The acoustic properties of granular materials with pore size distribution close to log-normal. *J. Acoust. Soc. Am.*, *110*[5], 2371–2378. https://doi.org/10.1121/1.1408312
32. NP-EN 993-1:2000. (2000) Ensaio das propriedades geométricas dos agregados, Parte 1: Análise Granulométrica, Método de Peneiração, IPQ, Lisboa.
33. ISO 10534-2:2001. (2001) Acoustics—determination of sound absorption coefficient and impedance in impedance tube: Part 2. *Transfer-function method*, ICS17.140.01
34. Bonfiglio, P.; Pompoli, F. (2007) Comparison of different inversion techniques for determining physical parameters of porous media. In *ICA 2007*[1-6]. International Congress of Acoustics.
35. Umnova, O.; Attenborough, K.; Li, K. M. (2000) Cell model calculations of dynamic drag parameters in packings of spheres. *J. Acoust. Soc. Am.*, *107*[6], 3113–3119. https://doi.org/10.1121/1.429340